EFFECTS OF MAGNETISM ON POROUS RECTANGULAR FINS WITH CONVECTION AND RADIATION

Sharif Ullah[a], Obaid J. Algahtani[b] Zia Ud Din[c] and Amir Ali[a,*]

[a]*Department of Mathematics, University of Malakand Chakdara Dir(L), Khyber Pakhtunkhwa, Pakistan*
[b] *Department of Mathematics, College of Sciences, King Saud University, Riyadh 11451, Saudi Arabia*
[c]*Higher Education, Archives and Libraries Department, Khyber Pakhtunkhwa, Pakistan*

Abstract

A fin is an extended surface used to enhance the surface area of a heat transfer surface between a hot source and the outside environment. To maximise the rate of heat transportation, the exterior surface of heated equipment is equipped with fins of various geometries. Heat is exchanged using fins in radiators, refrigeration systems, superheaters, combustion engines, electrical equipment, electric transformers, space vehicles, and aircraft engines. Reflecting these applications, we analyse the effect of a magnetic field on the thermal properties of radiating porous rectangular fins. The proposed model is numerically analysed using the shooting method under the influence of radiation and convection, then compared with the DTM solution and both the solution found closer to each other. The effect of various dimensionless parameters on temperature transmission in magnetized rectangular-shaped porous fins is revealed using numerical results. It is revealed that, when the Raleigh, Hartmann, Peclet numbers, convective and radiative parameters increase, the fin's thermal profile decreases, whereas the thermal profile increases with an increase in surface temperature, porosity, and ambient temperature. It is observed that the magnetic effect increases the heat transfer rate from porous rectangular fin surfaces. Accordingly, efficiency increases as Hartmann number, Raleigh number, and radiative parameter rise. Increasing Peclet number, surface temperature, and ambient temperature leads to a reduction in efficiency.

Keywords: Rectangular fin; Magnetic field; Convection; Heat generation; Radiation.

1. Introduction

In engineering applications, various fin structures are widely used to elevate heat transportation within the temperature limits of the systems. The investigation of fins is applicable to multiple appliances such as air conditioners, gas turbines, refrigeration, gas turbines, automobiles, electrical chips, vehicle radiators, and CPUs [1–4]. In this mechanism, heat is first transferred by conduction to the surface of the fins and then transported through convection and radiation to the outside medium. Here, we investigate magnetised porous rectangular fins for escalation of efficiency and heat transfer.

In various engineering appliances, nanofluids and cooling fluids were used to enhance heat transmission [5, 6]. To provide valuable thermal performance in various cooling processes, researchers use fins of different geometrical shapes. When the effectiveness of circular and star-shaped fins is compared, it is discovered that heat transfer through star-shaped fins increases more than heat transfer through annular fins [7]. Through experimental and mathematical results, the behaviour of a W-shaped fin was compared to that of straight parallel plate fins [8]. The thermal influences of longitudinal fins with a trapezoidal profile are investigated [9]. Heat loss through rectangular fins with low Reynolds numbers and forced convection was investigated using numerical and experimental results [10]. The enhancement in heat transfer from the rectangular extended surfaces was determined experimentally through an Electrohydrodynamics method [11]. The non-Fourier influence on the thermal transfer problem of fins was numerically described using

*Corresponding author: amiralishahs@yahoo.com

the Boltzmann method [12]. Thermal properties and entropy production in moving exponential and rectangular fins considering variable thermal conductivity were numerically discussed by [13]. It has been concluded that the entropy of exponential fins is higher than that of rectangular fins.
The porous extended mediums are made up of high thermal conductivity substances such as metal foams, which enhance thermal transfer [14]. Recently, the effectiveness of thermal systems, i.e., inflated power semiconductors, heat exchangers, photovoltaic-thermal and thermal insulators, etc., has been improved by including the porous parameter in fins [15–17]. Many researchers were interested in improving various systems using porous fins. Based on an analytical methodology, [18] analyses the effects of Peclet number, thermal transmission parameters, and moving conditions on the efficiency of a convecting longitudinal-type porous fin. To demonstrate regular heat loss by porous fins, [19] proposed a weighted residual method. They concluded that the capability of the fin is enhanced through amplifying porosity and also by enhancing the Darcy, Nusselt, and Rayleigh numbers of the fin. In the study by [20], the least squares method was used as a tool for examining the heat distribution involved in different types of longitudinal fins, accounting for porosity and variable heat generation. They obtained comparative results due to thermal transfer parameters like convection, conduction, and conduction in fin competence. In concentric tubes, the impact and significance of porous fins are examined for magnifying heat exchange utilising the finite volume method [21, 22]. They concluded that heat transmitter performance is highly impacted by thermal conductivity and fin spacing. The DTM has been used by [23] to present a heat exchange model of porous fins, which is assumed to be in motion. It has been revealed that Peclet number enhancement resulted in higher transmission of heat, and the rectangular fin is scrutinised as more effective as compared to the hyperbolic exchanger. The effects of gray gas radiation on the transfer of heat and mass in an annular cavity are analyzed numerically in [24]. Their numerical results indicate that gas radiation modifies flow structure, temperature, and concentration distributions in cavities. The [25] has numerically simulated the heat transfer and flow characteristics of a plate fin-and-tube heat exchanger along with slit fins on the ring bridge. The fin pitch was found to be the most significant factor affecting the heat transfer and flow characteristics of the ring-bridge slit fins, and reducing the front slit angle of the sample improved heat transfer. The effect of triangular ribs on the flow and heat transfer characteristics of a heat exchanger tube was presented in [26]. They reported that the performance evaluation criteria of the triangular rib enhanced tube can be improved by reducing the dimensionless pitch ratio and appropriately increasing the area of the triangular ribs.
The importance of the magnetic field on porous fin thermal exchange was studied in [27–29]. The work was further extended through the Adomian Decomposition Technique [30]. Further, in [31], the significant behaviour of the magnetic field on the effectiveness of porous fins for the transference of heat was carried out by applying the finite volume method. They found that enhancement of the magnetic field improved the heat transfer capability of fins. Then, the internal heat generation effect was added to the longitudinal fins' performance along with the magnetic field and analyzed by an iterative method [32]. The magneto-hydrodynamic impact on fins in different situations was studied in [33]. Time fractional order derivatives model are calculated using a caputo derivative in [34]. A comparison and analysis with other approaches demonstrate that the suggested approach is effective and precise. In [35], Fibonacci wavelet (FW) algorithms are used to approximate fractional order electrical circuits. Using the proposed method, electrical engineers are able to analyze and design fractional order systems with improved accuracy. An algorithm based on fractional order Fibonacci wavelets and block pulse functions is presented to solve the fractional Bagley-Torvik equation (BTE) [36]. In their numerical analysis, they demonstrate that their approach produces extremely precise results and is computationally more effective than previous ones. In [37], Wavelets collocation method is used for singularly perturbed differential–difference equations in control systems. It was found to be a reliable tool for solving SPDDEs in control systems through numerical experiments. A porous space is investigated numerically to determine the influence of variable density and magnetohydrodynamics on Williamson fluid [38]. They stated that the enhancing of the density variation parameter confirmed the reduction in velocity field and an increase in temperature of the fluid, while when the Williamson fluid parameter increased, both fluid velocity and temperature increased correspondingly. In [39, 40], the thermal case study on non-Newtonian fluids magnetized thermally and first-order chemical reactions was conducted. In this study the researchers found that for Eckert, Prandt numbers, curvature, heat generation, and Casson fluid parameters, the Nusselt number is higher in the presence of thermal radiation, whereas for positive variations in thermal conductivity, it is the opposite.
To investigate the effect of magnetic field and convection on radial porous fins with radiation, [41] applied the Runge Kutta method. They also presented the problem with a magnetic field versus the model without a magnetic field and concluded that the magnetic field improved the performance of the radial fin surface. The combined effects of thermal

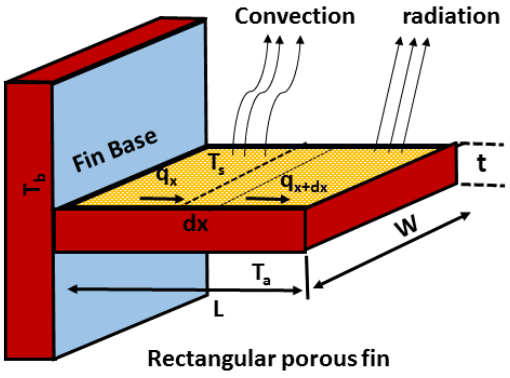

Figure 1: **Schematic diagram of a magnetised porous rectangular fin.**

radiations and temperature-dependent thermal conductivity are studied in stagnation point magnetized Casson fluid flow [42, 43]. The authors reported that higher thermal radiation values result in increased temperature of the Casson fluid, while positive variations in variable thermal conductivity result in greater temperature.
The significance of stretching or shrinking effects on rectangular fins is comparatively studied using existing different parameters with non-stretching rectangular fins by [44]. As measured in this study, the fin's performance decreases with stretching, while it provides high effectiveness when shrinking. Further, [45] applied the stretching/shrinking mechanism to different fin profiles with moving effects for valuable results. [46] considered the exponential fin model with stretching/shrinking effects for a numerical investigation of better thermal exchange. Later, in study [47], the performance of shrinking and stretching fins of a rectangular profile considering radiation is numerically examined, implying shooting technique, and then compared with the analytical solution of the differential transform method for validation.
Here, the uniform magnetic field is considered in the radiating, porous, and convecting rectangular-shaped fin. The governing equation is converted into a non-dimensionalized form, and then the numerical solution is obtained to interpret the behaviour of including parameters on a magnetised fin graphically.

2. Problem Formulation

As illustrated in Figure 1, we investigate heat exchange, convection, and radiation parameters using porous longitudinal rectangular fins of length L_f. A number of different parameters are used, including: h is a heat transfer coefficient, φ is porosity, T_s surface temperature, T_b shows fin base temperature, T_a ambient temperature, ρ density of fin material, and T temperature distribution. The emissivity of the material is ε, the specific heat is C_p, and the Stefan-Boltzmann constant is σ. It is important to note that fins have a fixed thermal conductivity k_a, a constant coefficient of heat transfer h for simplification of the model, and a uniform magnetic field is applied. Based on the assumption, the proposed model of the moving fin with a rectangular shape along with a porosity parameter, a heat-generating source, and thermal transmission via radiation and convection can be obtained in the form of [47–49].

$$q_x - \left[q_x + \frac{\partial q_x}{\partial x}dx\right] - hP_f(1-\varphi)\Big[T-T_a\Big]dx - \dot{m}C_p\Big[T-T_a\Big] - \varepsilon\sigma P_f\Big[T^4-T_s^4\Big]dx - \frac{J_{cd}\times J_{cd}}{\sigma}\Big[T-T_a\Big]dx = 0, \quad (1)$$

as $dx \to 0$, Eq. (1) becomes [32, 54]

$$\frac{\partial q_x}{\partial x} - hP_f(1-\varphi)\Big[T-T_a\Big] - \dot{m}C_p\Big[T-T_a\Big] - \varepsilon\,\sigma P_f\Big[T^4-T_s^4\Big] - \frac{J_{cd}\times J_{cd}}{\sigma}\Big[T-T_a\Big] = 0, \quad (2)$$

The mass flow rate $\dot{m}$ of the fluid flowing through the porous material can be written as

$$\dot{m} = \varphi\,\rho\,W\,v_w\,\triangle x, \quad (3)$$

where φ represents the porosity of the fin. The amount of φ ranges from 0 to 1 for a compact medium $\varphi = 0$. It should be stated that for $\varphi = 1$ no solid portion exist. Further, v_w correspond to the Darcy formula defined as [50]

$$v_w = \frac{\beta\, g K}{\nu}\Big[T - T_a\Big]. \tag{4}$$

The conduction current intensity J_{cd} can be written as

$$J_{cd} = \sigma\,(V \times B + E), \tag{5}$$

where J_{td} is the total current intensity which can be stated as

$$J_{td} = J_{cd} + \sigma V. \tag{6}$$

Using Fourier's law of heat conduction as

$$q_x = -k_{eff} A_f \frac{dT}{dx}, \tag{7}$$

where, k_{eff} indicates effective thermal conductivity.

$$\frac{d^2T}{dx^2} + \frac{U_f\,\rho\,C_p}{k_{eff}}\frac{dT}{dx} - \frac{hP_f(1-\varphi)}{A_f\,k_{eff}}\Big[T - T_a\Big] - \frac{\varepsilon\,\sigma\,P_f}{A_f\,k_{eff}}\Big[T^4 - T_s^4\Big] - \frac{J_{cd}\times J_{cd}}{\sigma} = 0. \tag{8}$$

Here the thermal diffusivity of the fin's material is given by $\lambda = k_{eff}/(\rho\,C_p)$.

$$\frac{J_{cd}\times J_{cd}}{\sigma} = \sigma\,B_0^2\,u^2. \tag{9}$$

Here, B_0 represents the magnetic field intensity. Using Eq. (9) in Eq. (8), we have

$$\frac{d^2T}{dx^2} + \frac{U_f\,\rho\,C_p}{k_{eff}}\frac{dT}{dx} - \frac{hP_f(1-\varphi)}{A_f\,k_{eff}}\Big[T - T_a\Big] - \frac{\varepsilon\,\sigma\,P_f}{A_f\,k_{eff}}\Big[T^4 - T_s^4\Big] - \frac{\sigma\,B_0^2\,u^2}{k_{eff}}\Big[T - T_a\Big] = 0. \tag{10}$$

Incorporating the following boundary conditions

$$At\ x = 0,\ T = T_b,\ \ \text{At}\ x = L_f,\ \frac{dT}{dx} = 0. \tag{11}$$

For non-dimensionalization, we consider

$$X = \frac{x}{L_f},\quad \theta = \frac{T}{T_b},\quad \theta_a = \frac{T_a}{T_b},\quad \theta_s = \frac{T_s}{T_b},\quad Ra = \frac{g\,\beta\,K\,t\Big[T_b - T_a\Big]}{\lambda\,\nu\,k_{eff}},\quad H = \frac{\sigma\,B_0^2\,u^2}{k_{eff}\,t},$$
$$Pe = \frac{U_f\,L_f}{\lambda},\quad N_r = \frac{\varepsilon\,\sigma\,P_f\,L_f^2\,T_b^3}{A_f\,k_{eff}},\quad N_c^2 = \frac{h\,(1-\varphi)\,P_f\,L_f^2}{A_f\,k_{eff}},$$

and obtained

$$\frac{d^2\theta}{dX^2} + Pe\frac{d\theta}{dX} - Ra\,\theta(X)^2 - N_c\Big[\theta(X) - \theta_a\Big] - N_r\Big[\theta(X)^4 - \theta_s^4\Big] - H\,\theta(X) = 0, \tag{12}$$

with boundary conditions

$$X = 0,\ \theta(X) = 1, \text{and}\ X = 1,\ \theta'(X) = 0. \tag{13}$$

It should be noted that Pe, Ra, N_c, H, N_r denotes Peclet number, Rayleigh number, convective parameter, Hartmann number, radiative parameter respectively.

3. The shooting method

The problem is solved using the shooting method. Shooting is a numerical technique for solving boundary value problems that consists of converting the boundary value problem into an initial value problem. To solve the corresponding initial value problem, the shooting method uses numerical techniques such as Euler and Runge-Kutta. The computed boundary value is then compared with the desired boundary value, and the initial guess is adjusted accordingly. Until a certain range of boundary values is achieved, the process is repeated. This method is useful when boundary conditions (BCs) are defined at both ends of an interval, but the solution behaviour between them is unknown. In general, we describe multiple paths until we identify the one with the best boundary value. Firstly, calculate the Dirichlet BVP of a linear differential equation.

$$\frac{d^2G}{dy^2} = F(y)\frac{dG}{dy} + L(y)\,G + M(y) \quad \text{subject to} \quad G(l) = \varepsilon, \quad G(m) = \gamma, \tag{14}$$

over the interval $[l,m]$, where, F and L are arbitrary functions and M is considered as the source term. The solution can be derived from the linear combination of the functions $\varphi(y)$ and $\mu(y)$, which are also the solutions to IVPs.

$$G(q) = \mu(q) + \frac{\gamma - \chi(m)}{\varphi(m)} \cdot \varphi(q), \tag{15}$$

where $\chi(q)$ is the IVP solution.

$$\frac{d^2\chi}{dq^2} = p(q)\frac{d\chi}{dq} + s(q)\,\chi + h(q), \quad \text{subject to} \quad \chi(l) = \varepsilon, \frac{d\chi(l)}{dq} = 0. \tag{16}$$

Similarly, $\varphi(q)$ is another initial value problem solution.

$$\frac{d^2\varphi}{dq^2} = p(q)\frac{d\varphi}{dq} + s(q)\,\varphi + h(q), \quad \text{subject to} \quad \varphi(l) = \varepsilon, \frac{d\varphi(l)}{dq} = 0. \tag{17}$$

4. Differential Transform Method (DTM)

For understanding fundamentals of DTM, let $\phi(x)$ is an analytic function in the domain D and $y = y_i$ represents an arbitrary point. A function $\psi(z)$ can be expressed by a power series with its centre at z_i. The expansion of $\psi(z)$ can be written as [51]

$$\Psi(\ell) = \frac{1}{\ell!}\left[\frac{d^\ell \psi(y)}{dy^\ell}\right]_{y=y_\ell} \quad \forall y \in D, \tag{18}$$

The Maclaurin series for a function $\psi(y)$ can be obtained by putting $y_\ell = 0$ in Eq.(18)

$$\psi(y) = \sum_{\ell=0}^{\infty} (y - y_i)^\ell\, \psi(\ell) \quad \forall y \in D. \tag{19}$$

The differential transformation of $\psi(y)$ gives [52]

$$\Psi(\ell) = \sum_{\ell=0}^{\infty} \frac{(y - y_i)^\ell}{\ell!}\left[\frac{d^\ell \psi(y)}{dy^\ell}\right]_{y=y_i}, \tag{20}$$

where $\psi(y)$ represents a primary function and $\Psi(\ell)$ is transform function. The differential spectrum $\Psi(\ell)$ is bounded by an interval $y \in [0,M]$, where $M \in \mathscr{R}$.

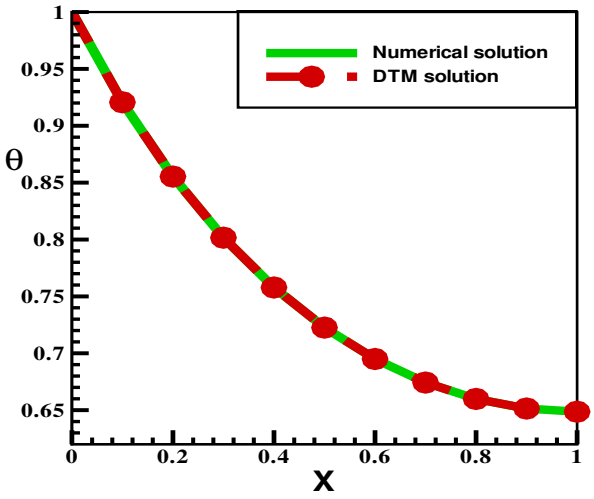

Figure 2: **Comparison between DTM and numerical solutions.**

5. Applications of Differential Transform Method

To evaluate model (12), we apply DTM as discussed in previous section and rearranging the terms, we obtain

$$\begin{aligned}\Theta(\ell+2) &= \frac{1}{(\ell+1)(\ell+2)}\Bigg[-Pe\,(\ell+1)\,\Theta(\ell+1)+R_a\sum_{c=0}^{b}\Big[\Theta(c)\,\Theta(b-c)\Big]-N_r\,\theta_s\,\delta(\ell)+(N^2+H)\,\Theta(\ell)\\ &\quad +N_r\sum_{a=0}^{\ell}\sum_{b=0}^{a}\sum_{c=0}^{b}\psi(c)\phi(b-c)\phi(a-b)\phi(\ell-a)-N^2\,\theta_a\delta(\ell)\Bigg]. \qquad (21)\end{aligned}$$

The boundary conditions can be transformed as

$$\Theta(0)=\gamma, \quad \Theta(1)=1. \qquad (22)$$

Similarly

$$\Theta(2) = \frac{1}{2}\Big[(N_c+H)\,a-N_r\,\theta_s^4-N_c\,\theta_a+Nr\,a^4-Pe+R_a\,\gamma^2\Big], \qquad (23)$$

$$\Theta(3) = \frac{1}{6}\Big[N_c+H+N_r\,(4\,\gamma^3+\gamma^4)-2\,Pe\,\Theta(2)+\gamma R_a\,(-\gamma+1)\Big], \qquad (24)$$

$$\Theta(4) = \frac{1}{12}\Big[(N_c+H)\Theta(2)+N_r(4\gamma^3+4\gamma^3\Theta(2)+\gamma^4+6\gamma^2)-3Pe\Theta(3)\Big]+R_a\Big[2\gamma\Theta(2)-2\gamma+1+2\gamma^2\Big], \qquad (25)$$

$$\begin{aligned}\Theta(5) &= \frac{1}{20}\Big[(N_c+H+4N_r\,\gamma^3)\Theta(3)+N_r\big[(4\,\gamma^3+12\,\gamma^2)\,\Theta(2)+\gamma^4\\ &\quad +6\,\gamma^2+4\,\gamma^3+4\,\gamma\big]-4\,Pe\,\Theta(4)+R_a\Big[2\,\gamma\Theta(3)-2\,\Theta(2)-2\,\gamma\Theta(2)+\gamma-\frac{1}{6}\,\gamma^2\Big]\Big]. \qquad (26)\end{aligned}$$

The final solution can be written as

$$\theta(x)=\sum_{l=0}^{n}\Theta(l)x^l. \qquad (27)$$

The numerical solution are compared with DTM solution in Figure 2, where good agreement is obtained.

6. Results and Discussion

Various parameters are used to investigate the heat transfer in magnetised porous rectangular fins. The thermal profile $\theta(x)$ for six dimensionless parameters is computed, and the results are presented graphically. The curves shown are obtained by evaluating the code of the final solution provided through shooting technique using "Mathematica Software" code and furnished by using "Tecplot software". As shown in Figure 3(a), temperature distribution steps up with boosted ambient temperature. Increasing θ_a leads to a decline in convection heat loss, which results in a higher temperature at the fin's surface. Similarly, Figure 3(b) shows that the thermal profile rises when the surface temperature θ_s value becomes higher because a low amount of heat is absorbed from the magnetised fin surface when the surrounding temperature and surface temperature are raised. In actuality, as θ_a and θ_S increase, less convective heat is dissipated from the moving fin's surface, which maintains greater temperatures at the fin's exterior.

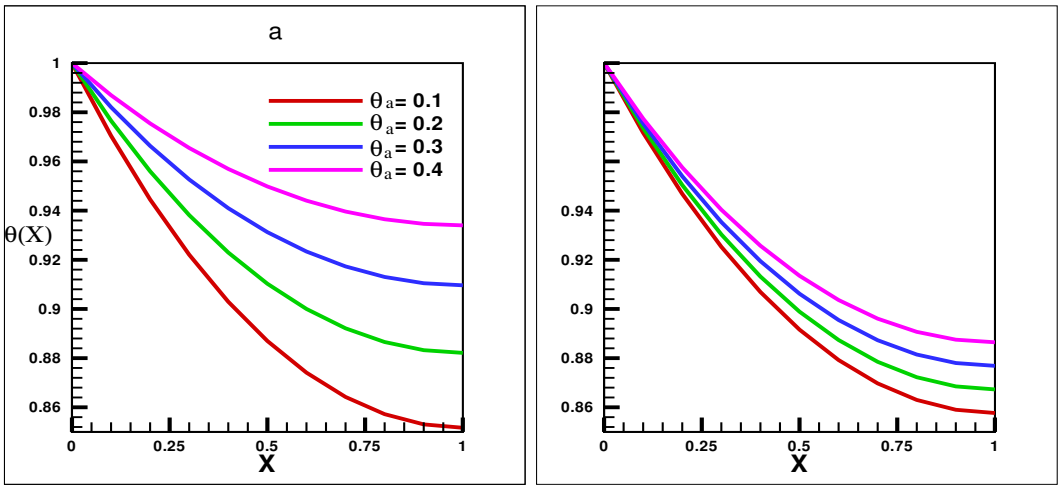

Figure 3: **Thermal distribution computation for magnetised rectangular fin at θ_a and θ_S.**

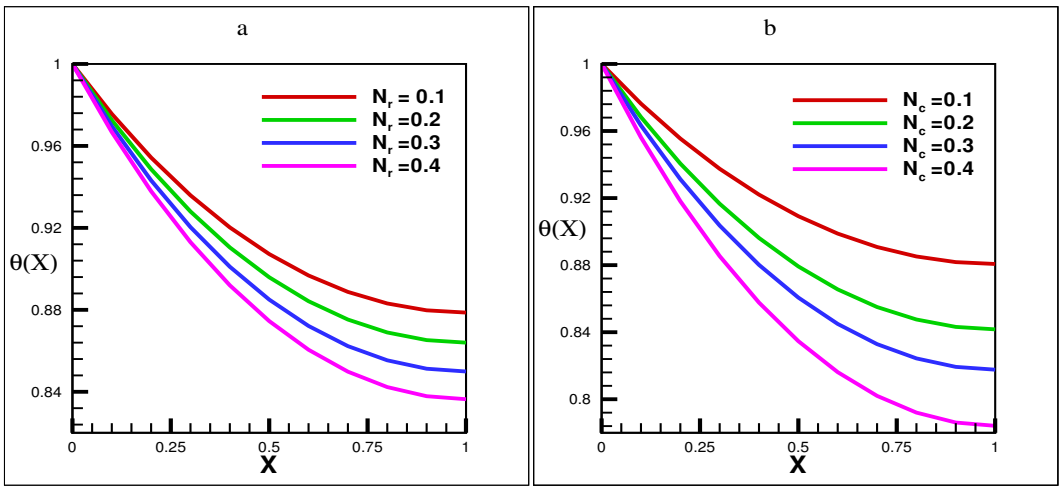

Figure 4: **Thermal distribution computation for magnetised rectangular fin at N_r and N_c.**

Fig. 4(a) demonstrated the temperature profile behaviour versus length of the magnetised porous fin with the impact of the radiative parameter N_r. Clearly, by increasing the radiative parameter N_r, the temperature profile diminishes. Physically, heat is carried from the fin surface by radiation, causing the temperature profile to step down.

Thermal transmission improves when the radiative parameter rises. Also, the effect of the convective parameter N_c on the temperature profile behaviour of the magnetised fin is depicted in Figure 4(b), which illustrates that the thermal profile lowers with the growing convective parameter. Because of the convection effect surrounding the fin, more heat is lost from the fin, and it gets colder. Therefore, enhancement in heat transference occurs at the fin's surface with upgraded convective parameters.

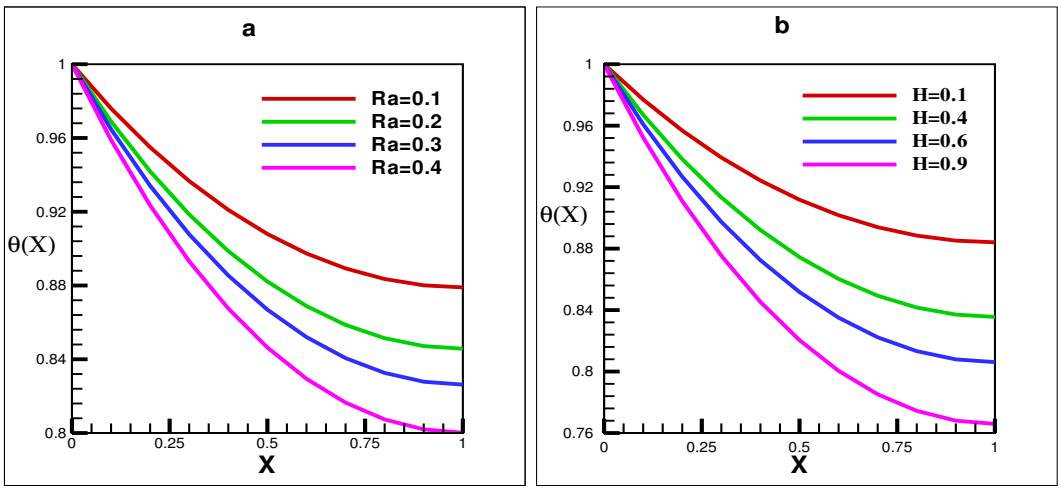

Figure 5: **Thermal distribution computation for magnetised rectangular fin at Ra and H.**

The thermal distribution of the porous magnetised fin is due to the effects of the porous variable Ra value as displayed in Figure 5(a). It shows that the fin thermal profile highly diminishes with the upgrade of the porosity variable; consequently, high transmission of heat from the fin surface occurs. In fact, elevating the Raleigh number causes an increase in the relative permeability value of the magnetised porous fin, subsequently enhancing the penetration competence of single-phase fluid via the pores of the fin. This phenomenon resulted in intensifying the impact of the buoyancy force, and hence the fin started to convect more temperature. As a result, thermal transportation is enhanced by the magnetised fin. Similarly, Figure 5(b) portrays the Hartmann number H effect on the thermal profile of the fin. In the figure, thermal profile decay is observed when the Hartmann number increases, so heat loss from the magnetised fin increases. Because with ameliorating the Hartmann number or magnetic number, magnetic field strength steps up, which improves thermal convection. Thus, the temperature profile becomes lower.

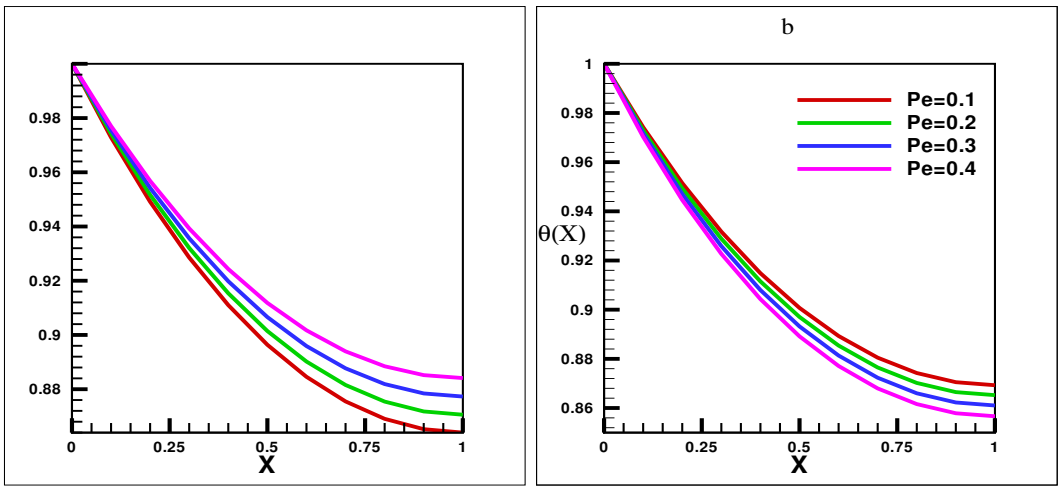

Figure 6: **Thermal distribution computation for magnetised rectangular fin at φ and Pe.**

The porosity number φ impact on the behaviour of the thermal profile of a magnetised fin is declared in Figure 6(a). It is exhibited that when the porosity number φ value enhances, the fin thermal profile grows. Figure 6(b) reveals the Peclet number or dimensionless speed influence on the temperature profile of the investigated fin. In fact, when Peclet number Pe grows, the movement of materials becomes faster, which means that in a very short time, materials on the fin are exposed to the outside medium, and hence heat loss from the fin surface improves. The cooling process takes longer when $Pe = 0$, which shows a static fin. As a result, temperatures are higher than when a fin is moving. It is therefore recommended to use a higher Peclet number when cooling is required.

Furthermore, various parameters are compared with the literature [32, 47, 53, 54]. According to their findings, the temperature profiles of rectangular, triangular, and trapezoidal fins decline as Hartmann number, porosity parameter, radiation, and convection parameters grow, but they rise as ambient temperature, Peclet number, and internal heat generation enhance. Figs. 3-6 also show the same result for rectangular fins considering magnetic field.

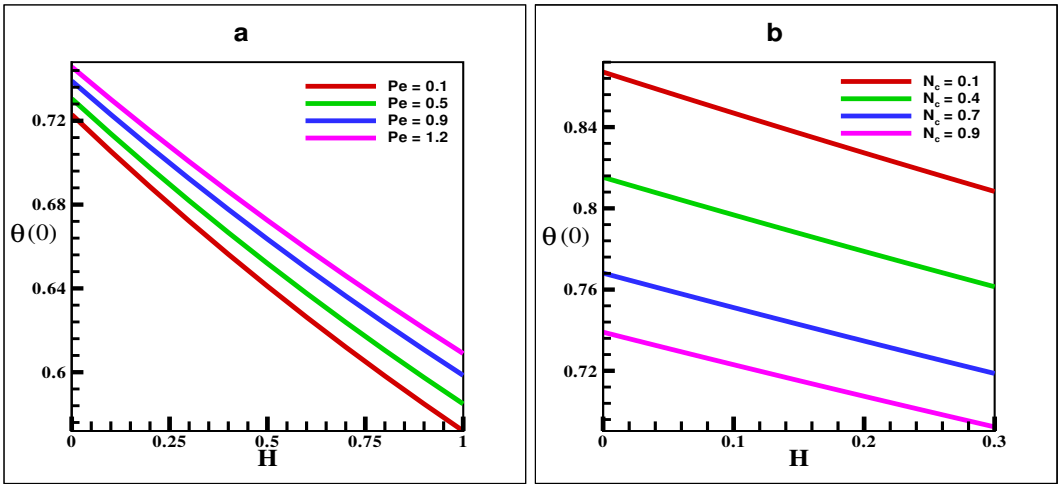

Figure 7: **Fin's tip temperature computation for a magnetised rectangular fin at Pe and N_c.**

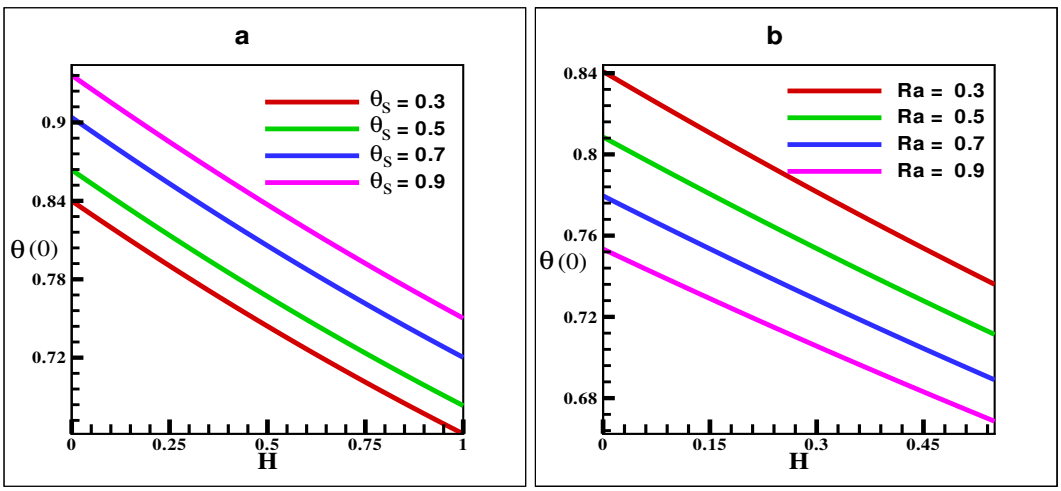

Figure 8: **Fin's tip temperature computation for a magnetised rectangular fin at θ_S and R_a.**

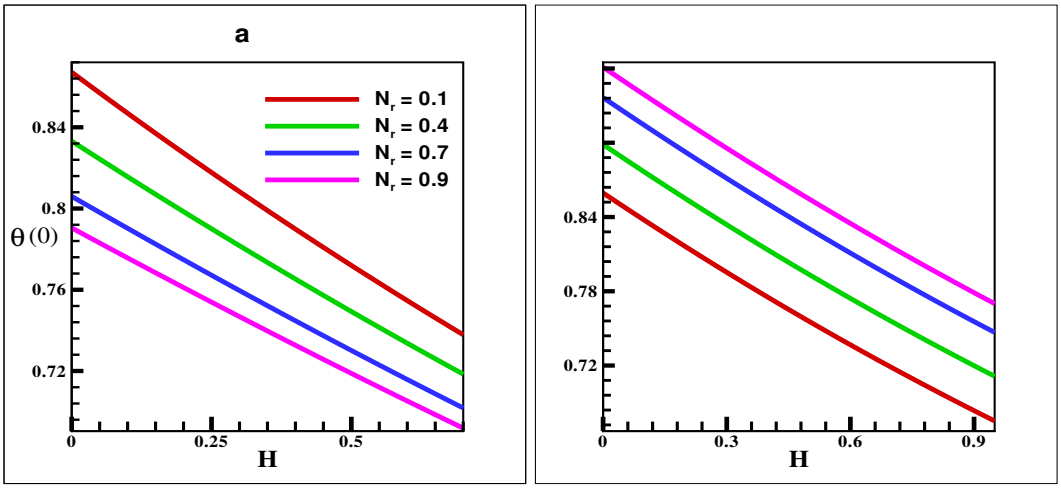

Figure 9: **Fin's tip temperature computation for a magnetised rectangular fin at N_r and θ_a.**

Further, Figures 7-9 illustrate the porous rectangular fin's tip temperature along the Hartmann number. These figures demonstrate the repercussions of Hartmann number, showing that the rectangular fin's tip temperature decreases as Hartmann number increases. Figs. 7(a) and 7(b) show that fin's tip temperature is exceeding due to amplifying P_e from 0.1 to 1.2 and decreasing due to enhancing N_c from 0.1 to 0.9. In addition, Figures 8(a) and 8(b) show that the tip temperature upgrades when θ_s increases from 0.3 to 0.9, while the outcome is contrasted when Ra increases from 0.3 to 0.9. In Figure 9(a), amplification of N_r causes a reduction in the fin's tip temperature, while θ_a improvement causes a rise in the fin's temperature, as displayed in Figure 9(b).

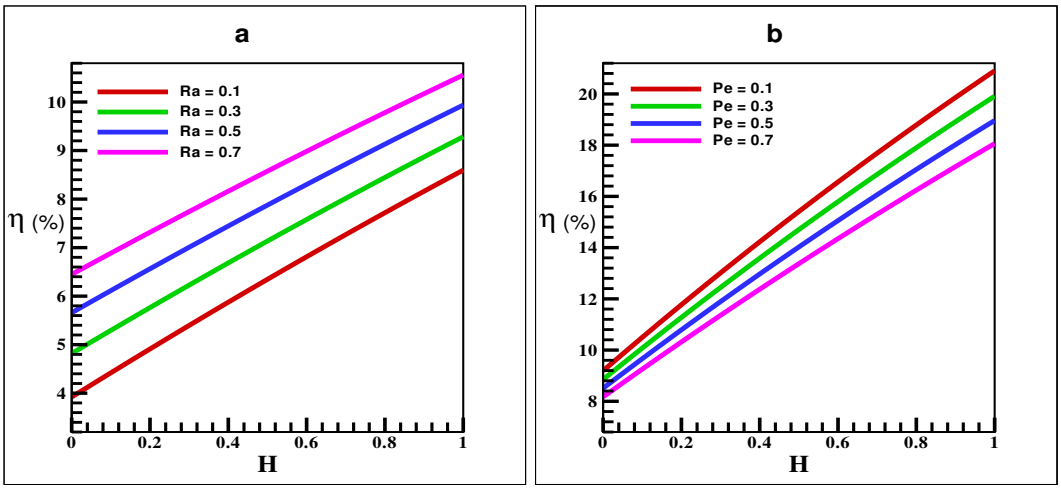

Figure 10: **Efficiency computation for a magnetised rectangular fin at Ra and Pe.**

The efficiency along with the Hartmann number for a porous rectangular fin with considered parameters can be seen in Figures 10-12. These figures show a rise in fin efficiency with the amplification of Hartmann number H. Furthermore, increasing N_r and R_a from 0.1 to 0.7 causes the efficiency η to increase, as shown in Figures 10(a) and 11(a). Figs. 10(b), 11(b), 12(a), and 12(b) demonstrate the declining efficiency η, resulting from a continuous increase of Pe from 0.1 to 0.7, θ_S from 0.3 to 0.95, θ_a from 0.1 to 0.7, and N_c from 0.1 to 0.16.

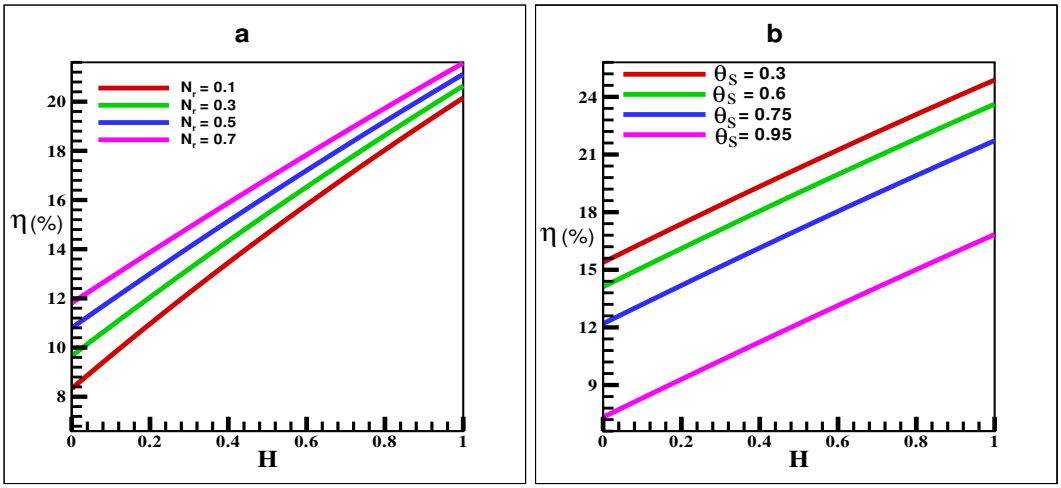

Figure 11: **Efficiency computation for magnetised rectangular fin at N_r and θ_S.**

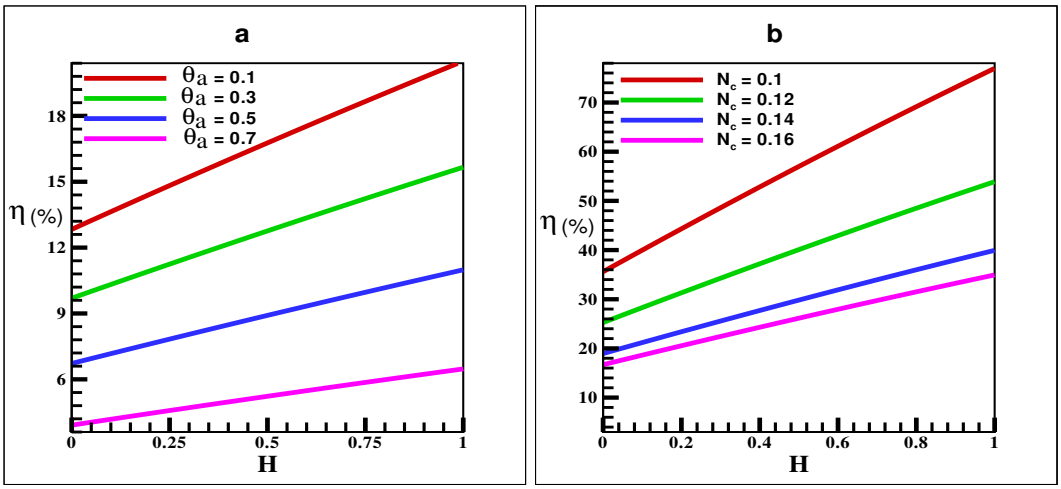

Figure 12: **Efficiency computation for a magnetised rectangular fin at θ_a and N_c.**

As the physical effects of the porous parameter R_a, convection N_c, radiation N_r, and magnetic number H increase, the temperature distribution declines as these parameters are subtracted from the equation. The mathematical equation therefore validates the physical parameters. From the above results, it is clear that with the enhancement of uniform magnetic field, porosity parameter and radiation parameter increases the heat transfer and efficiency of the fin.

7. Comparison with Experimental Results

In order to validate the results with the experimental published results. In experimental analysis [55], fin porosity affects heat transfer. As the number of perforations increases (24 to 60), the heat dissipation rate increases by 20% to 70% . Further increases in perforation numbers result in a reduction of fin heat dissipation. Experimentally, annular porous fins attached to a heated vertical cylinder were investigated in [56]. With a 10 mm thick fin, the heat transfer coefficient was enhanced by 7.9%, and with a porous layer, it was enhanced by 131%. In this study, porous fins were found to improve heat transfer significantly. The thermal performance of an annular fin-shell tube storage system using magnetic fluid is experimentally investigated in [57]. When a magnetic fluid is added to an annular fin geometry, the

fin efficiency increases by 20%. In this study, the magnetic ring of a small magnet with a thickness of 1 mm and a diameter of 2.5 mm was used to maintain the thin layer of magnetic fluid on the fins. With a thin magnetic fluid layer over the top surface of the fin, the relative heat transfer rate is significantly enhanced 35%, resulting in a significant improvement in fin performance. Furthermore, the temperature distribution along the length of the fin shows a sharp decline. The present numerical results illustrates the similar trend with the experimental study.

8. Conclusions

The thermal study of magnetised, porous, and moving rectangular fins suggesting mechanisms of convection and radiation is addressed. The temperature profile of the fin is numerically analysed by shooting method via graphical plots for considering parameters. The numerical result is compared with the DTM solution and good agreement is observed. The investigated results declared that the temperature profile upgrading occurs by growing ambient temperature, surface temperature, and porosity number, but when a radiative parameter, a convective parameter, the Raleigh number, the Hartmann number (a magnetic number), and the Peclet number enhance, the fin's temperature profile declines. The rectangular fin's tip temperature decreases as the Hartmann number, Raleigh number, and radiative parameters grow. In contrast, as ambient temperature, surface temperature, and Peclet number rise, the fin's tip temperature increases. When the Hartmann number is continuously increasing, rectangular fins' efficiency improves. Furthermore, efficiency becomes higher with an increase in the Raleigh number and radiative parameter but depreciates with an increase in surface temperature, ambient temperature, and Peclet number. When the magnetic field strength is exposed to a rectangular-shaped moving porous fin, along with the impacts of radiative and convective parameters, the thermal dissipation and effectiveness of the investigated model are extensively stepped up for significant performance. The current thermal study of magnetised rectangular fins inserting relevant thermal factors will be used to improve the capabilities of many technological appliances.

Nomenclature

A_f	Area of fin's surface $[m^2]$	Pe	Peclet parameter $(= U_f L_f/\lambda), [-]$
B	Magnetic Induction $[kgs^{-2}A^{-1}]$	P_f	Fins perimeter $[m]$
B_0	Magnetic field intensity	q_x	Heat transfer rate $[Jm^{-2}]$
C_p	Specific heat coefficient $[Jkg^{-1}K^{-1}]$	Ra	Rayleigh number $(= Gr \cdot Pr), [-]$
E	Electric field $[kgms^{-3}A^{-1}]$	T	Fin temperature $[K]$
g	Gravity constant $[ms^{-2}]$	t	Fin's base thickness $[m]$
h	Convective heat coefficient $[Jm^{-2}K^{-1}]$	T_b	Fin base temperature $[K]$
H	Hartmann number $(= \sigma B_0^2 u^2/k_{eff}t), [-]$	T_s	Dimensional surface temperature $[K]$
J_{td}	Total current density $[Am^{-2}]$	T_a	Dimensional ambient temperature $[K]$
J_{cd}	Conduction current density $[Am^{-2}]$	u	Axial velocity $[ms^{-1}]$
K	Fin permeability $[m]$	U_f	Speed of moving fin $[ms^{-1}]$
k_{eff}	Effective thermal conductivity $[Wm^{-1}K^{-1}]$	V	Voltage $[kgm^2s^3A^{-1}]$
L_f	Fins length $[m]$	v_w	velocity of the fluid flowing through the fin $[ms^{-1}]$
$\dot{m}$	Mass flow rate $[kgs^{-1}]$	W	Width of the fin $[m]$
N_r	Radiation parameter $(= \varepsilon\sigma L_f^2 T_b^3/k_{eff}A_f), [-]$	X	Dimensionless distance $(= x/L_f), [-]$
N_c	Convection parameter $(= hP_f L_f^2/K_{eff}A_f), [-]$	x	Dimensional distance $[m]$
G_r	Grashof number $(= \beta g(T-T_a)L_f^3/\nu^2), [-]$	P_r	Dimensional distance $(= \nu/\lambda), [-]$
M	Variable	R	Real numbers

Greek symbols

θ_s – Dimensionless surface temperature $(= T_s/T_b), [-]$ θ_a – Dimensionless ambient temperature $(= T_a/T_b), [-]$

β – Volumetric thermal expansion coefficient $[Wm^{-1}K^{-1}]$ ν – Kinematics viscosity $[m^2s^{-1}]$

θ – Dimensionless temperature of the fin $(= T/T_b), [-]$ φ – Fin's porosity $[m]$

ρ – Density of material $[kgm^{-3}]$ ε – Surface emissivity $[Wm^{-2}]$

λ – Thermal diffusivity $[m^2s^{-1}]$ η – Fin's efficiency

Subscripts

a – Ambient property eff – Porous properties

c – Convection s – Surface of the fin

b – Base of the fin f – Fin

Abbreviations

IVP – Initial value problem $SPDDES$ – Singularly perturbed differential–difference equations

BCs – Boundry conditios DTM – Differential Transform Method

CPU – Central processing unit BVP – Boundry value problem

Declarations

Conflict of interest: It is declared that all authors have no conflict of interest regarding this manuscript.
Authors Contribution: It is also declared that all the authors have equal contribution in the manuscript. Further, the authors have checked and approved the final version of the manuscript.
Availability of Data and Material: The data regarding this manuscript is available within the manuscript.
Acknowledgement: Researchers Supporting Project number (RSP2024R447), King Saud University, Riyadh, Saudi Arabia.

References

[1] Kraus, A.D., *et al.*, *Extended Surface Heat Transfer*, John Wiley, Inc., New York, 2001.
[2] Kalpakjian, S., *Manufacturing Engineering and Technology*, Pearson Education, India, 2001.
[3] Shi, Y., *et al.*, Robust optimization design of a flying wing using adjoint and uncertainty-based aerodynamic optimization approach, *Struct. Multidisc. Optim.*, *66* (2023), 110, pp. 1-21.
[4] Yang, W., *et al.*, Phase-field simulation of nano-α' precipitates under irradiation and dislocations, *J. Mater. Res. Technol.*, *22* (2023), pp. 1307-1321.
[5] Luo, G., *et al.*, Highly Stretchable, Knittable, Wearable Fiberform Hydrovoltaic Generators Driven by Water Transpiration for Portable Self-Power Supply and Self-Powered Strain Sensor, *Small*, *20* (2024), 12, pp. 2306318.
[6] Zhu, C., Optimizing and using AI to study of the cross-section of finned tubes for nanofluid-conveying in solar panel cooling with phase change materials, *Eng. Anal. Bound. Elem.*, *157* (2023), pp. 71-81.
[7] Mladen, B., Experimental testing of the heat ex-changer with star-shaped fins, *Int. J. Heat and Mass Transf.*, *149* (2020), pp. 119190,.
[8] Zhang, K., *et al.*, Experimental and numerical investigation of natural convection heat transfer of W-type fin arrays, *Int. J. Heat and Mass Transf.*, *152* (2020), pp. 119315.
[9] Turkyilmazoglu, M., Efficiency of the longitudinal fins of trapezoidal profile in motion, *J. Heat Transf.*, *139* (2017), pp. 094501.
[10] Adhikari, R. C., *et al.*, An experimental and numerical study of forced convection heat transfer from rectangular fins at low Reynolds numbers, *Int. J. Heat and Mass Transf.*, *163* (2022), pp. 120418.
[11] Rezaee, M., *et al.*, Experimental study of natural heat transfer enhancement in a rectangular finned surface by EHD method, *I. J. Comm. Heat Mass Transf.*, *119* (2020), pp. 104969.
[12] Liu, Y., *et al.*, Numerical simulation of non-Fourier heat conduction in fins by lattice Boltzmann method, *Applied Therm. Eng.*, *166* (2020), pp. 114670.
[13] Din, Z. U., *et al.*, Entropy generation from convective–radiative moving exponential porous fins with variable thermal conductivity and internal heat generations, *Scientific Reports*, *12* (2022), pp. 1-11.
[14] Maghsoudi, P., Siavashi, M., Application of nanofluid and optimization of pore size arrangement of heterogeneous porous media to enhance mixed convection inside a two-sided lid-driven cavity, *J. Therm. Anal. Calorim.*, *135* (2019), pp. 947–961.

[15] Aminian, E., *et al.*, Magnetic field effects on forced convection flow of a hybrid nanofluid in a cylinder filled with porous media: a numerical study, *J. Therm. Anal. Calorim.*, *141* (2020), pp. 2019–2031.
[16] Aminian, E., *et al.*, Investigation of forced convection enhancement and entropy generation of nanofluid flow through a corrugated minichannel filled with a porous media, *Entropy*, *22* (2020), pp. 1008.
[17] Moghadasi, H., *et al.*, Numerical analysis on laminar forced convection improvement of hybrid nanofluid within a U-bend pipe in porous media, *Int. J. Mech. Sci.*, *179* (2020), pp. 105659.
[18] Dogonchi, A. S., Ganji, D. D., Convection–radiation heat transfer study of moving fin with temperature-dependent thermal conductivity, heat transfer coefficient and heat generation, *Appl. Therm. Eng.*, *103* (2016), pp. 705–712.
[19] Sobamowo, M. G., Thermal analysis of longitudinal fin with temperature-dependent properties and internal heat generation using Galerkin's method of weighted residual, *Appl. Therm. Eng.*, **99** (2016), pp. 1316–1330.
[20] Shateri, A. R., Salahshour, B., Comprehensive thermal performance of convection–radiation longitudinal porous fins with various profiles and multiple nonlinearities, *Int. J. Mech. Sci.*, *136* (2018), pp. 252–263.
[21] Logesh, K., *et al.*, Numerical investigation on the possibility of heat transfer enhancement using reduced weight fin configuration, *Int. J. Ambient Energy*, *41* (2018), pp. 142–145.
[22] Gao, S., *et al.*, Extremely compact and lightweight triboelectric nanogenerator for spacecraft flywheel system health monitoring, *Nano Energy*, 122 (2024), pp. 109330.
[23] Din, Z. U., *et al.*, Heat transfer analysis: convective-radiative moving exponential porous fins with internal heat generation. *Math. Biosci. Eng.*, *19*, (2022), pp. 11491-11511.
[24] Boussandel, A., *et al.*, Numerical analysis of gray gas radiation effects on heat and mass transfer in an annular cavity, *Thermal Science*, (2023), pp. 114-124.
[25] Wang, Z., Ouyang, X., Numerical simulation of heat transfer and flow characteristics for plate fin-and-tube heat exchanger with ring-bridge slit fins, *Thermal Science*, (2023), pp. 86-96.
[26] Shiquan, Z.H., *et al.*, Effect of triangular ribs on the flow and heat transfer characteristics of heat exchanger tube, *Thermal Science*, *28* (2024).
[27] Hoshyar, H. A., *et al.*, Least square method for porous fin in the presence of uniform magnetic field, *J. applied fluid mech.*, *9*, (2016), pp. 661-668.
[28] Li, X., *et al.*, Non-contact manipulation of nonmagnetic materials by using a uniform magnetic field: Experiment and simulation, *Journal of Magnetism and Magnetic Materials*, 497, (2020), pp. 165957.
[29] Dong, Z., *et al.*, Magnetic field effect on the sedimentation process of two non-magnetic particles inside a ferrofluid, *Journal of Magnetism and Magnetic Materials*, 589 (2024), pp. 171501.
[30] Patel, T., Meher, R., Thermal Analysis of the porous fin with uniform magnetic field using Adomian decomposition Sumudu transform method, *Nonlinear Eng.*, *6* (2017), pp. 191-200.
[31] Oguntala, G., *et al.*, Transient thermal analysis and optimization of convective-radiative porous fin under the influence of magnetic field for efficient microprocessor cooling, *I. J. Therm. Sci.*, *145* (2019), pp. 106019.
[32] Oguntala, G., *et al.*, Efficient iterative method for investigation of the convective–radiative porous fin with internal heat generation under a uniform magnetic field, *I. J. Applied Comp. Math.*, *5*, (2019), pp. 1-13.
[33] Sreedevi, P., Reddy, P.S., Effect of SWCNTs and MWCNTs Maxwell MHD nanofluid flow between two stretchable rotating disks under convective boundary conditions, *Heat Transf.—Asian Res.*, *48* (2019), pp. 4105-4132.
[34] Yadav, P., *et al.*, Fibonacci wavelet method for time fractional convection–diffusion equations, *Math. Methods Applied Sci.*, *47* (2024), pp. 2639-2655.
[35] Shahid, A., *et al.*, An efficient method for the fractional electric circuits based on Fibonacci wavelet, *Results in Physics*, *52* (2023), pp. 106753.
[36] Yadav, P., *et al.*, Solving fractional Bagley-Torvik equation by fractional order Fibonacci wavelet arising in fluid mechanics, *Ain Shams Eng. J.*, *15* (2024), pp. 102299.
[37] Shahid, A., *et al.*, Wavelets collocation method for singularly perturbed differential–difference equations arising in control system, *Results Applied Math.*, *21* (2024), pp. 100415.
[38] Abbas, A., *et al.*, Numerical simulation of variable density and magnetohydrodynamics effects on heat generating and dissipating Williamson Sakiadis flow in a porous space: Impact of solar radiation and Joule heating, *Heliyon*, *9* (2023), pp. 1-16.
[39] Rehman, K. U., *et al.*, Features of Casson liquid in non-linear radiative magnetized cylindrical media: a numerical solution, *Waves in Random and Complex Media*, (2022), pp. 1–18.
[40] Rehman, K.U., *et al.*, A comparative thermal case study on thermophysical aspects in thermally magnetized flow regime with variable thermal conductivity, *Case Stud. Therm. Eng.*, *44* (2023), pp. 102839.
[41] Din, Z. U., *et al.*, Entropy generation from convective–radiative moving exponential porous fins with variable thermal conductivity and internal heat generations, *Scientific Reports*, *12* (2022), pp. 1-11.
[42] Rehman, K.U., *et al.*, Mutual impact of thermal radiations and temperature dependent thermal conductivity on non-newtonian multiple flow regimes, *Case Stud. Therm. Eng.*, *42* (2023), pp. 102752.
[43] A. Rehman, *et al.*, Stability analysis of the shape factor effect of radiative on MHD couple stress hybrid nanofluid, *South African Journal of Chemical Engineering*, 46 (2023), pp. 394-403.
[44] Turkyilmazoglu, M., Stretching/shrinking longitudinal fins of rectangular profile and heat transfer, *Energy Conversion Manag.*, *91* (2015), pp. 199-203.
[45] Mosavat, M., *et al.*, Heat transfer study of mechanical face seal and fin by analytical method, *Eng. Sci. Tech.*, *21* (2018), pp. 380–388.
[46] Gireesha, B. J., *et al.*, Effects of stretching/shrinking on the thermal performance of a fully wetted convective-radiative longitudinal fin of exponential profile, *App. Math. Mech.*, *43* (2022), pp. 389–402.
[47] Din, Z. U., *et al.*, Investigation of heat transfer from convective and radiative stretching/shrinking rectangular fins, *Math. Prob. Eng.* (2022).
[48] Turkyilmazoglu, M., Efficiency of heat and mass transfer in fully wet porous fins: exponential fins versus straight fins, *Int. J. Refrig.*, *46*, (2014), pp. 158-164.

[49] Din, Z.U., *et al.*, Heat transfer analysis: convective-radiative moving exponential porous fins with internal heat generation. *Math. Biosci. Eng. 19*, (2022), pp. 11491-11511.
[50] Das, R., Ooi, K.T., Predicting multiple combinations of parameters for designing a porous fin subjected to a given temperature requirement, *Energy Convers. Manage.*, *66* (2013), pp. 211-219.
[51] Hussin, C., *et al.*, General differential transformation method for higher order of linear boundary value problem, *Borneo Science Journal*, *27*, (2010) pp. 35-46.
[52] Ghafoori, S., *et al.*, Efficiency of differential transformation method for nonlinear oscillation: comparison with HPM and VIM, *Curr. Appl. Phys.*, *11* (2011), pp. 965–971.
[53] Ullah, I., *et al.*, Heat transfer analysis from moving convection-radiative triangular porous fin exposed to heat generation, *Case Stud. Therm. Eng.*, *38* (2022), pp. 102177.
[54] Din, Z. U., *et al.*, Investigation of moving trapezoidal and exponential fins with multiple nonlinearities, *Ain Shams Eng. J.*, *14* (2022), 5, pp. 101959.
[55] Prasad, L., *et al.*, An experimental study of heat transfer enhancement in the perforated rectangular fin, *J. Integr. Sci. Technol.*, *4* (2016), 1, pp. 5-9.
[56] Kiwan, S., *et al.*, An experimental investigation of the natural convection heat transfer from a vertical cylinder using porous fins, *App. Therm. Eng.*, *179* (2020), pp. 115673.
[57] Pathak, S., *et al.*, Improved thermal performance of annular fin-shell tube storage system using magnetic fluid, *Applied energy*, *239* (2019), pp. 1524-1535.

Submitted: 15.02.2024.
Revised: 02.05.2024.
Accepted: 08.05.2024.